Aluminum(III) Interactions with the Acidic Amino Acid Chains

Jose M. Mercero, Joseph E. Fowler, and Jesus M. Ugalde*

Kimika Fakultatea, Euskal Herriko Unibertsitatea, P. K. 1072, 20080 Donostia, Euskal Herria, Spain

Received: February 16, 1998; In Final Form: June 17, 1998

We have performed an ab initio study of aluminum(III) cation with the aspartic and glutamic amino acid residues, i.e., the carboxylate group. Density functional theory methodology was used, and the covalent and noncovalent interactions were analyzed using natural bond orbital theory. First we have investigated the smallest functional moiety of these amino acids, the carboxylate anion. Additionally, we have sequentially introduced two methyl groups to more accurately represent the aspartic and glutamic acid chains. We have compared these data with the nontoxic metal cation, e.g., magnesium(II). Our calculations demonstrate that aluminum(III) binds much more tightly to the ligands than magnesium(II) and the addition of the methyl groups leads to stronger bonds, though the effect of the second methyl group is less than that of the first.

1. Introduction

Over the past several years, after numerous negative aspects of aluminum biological activity were reported,[1−7] the presence of aluminum in biological systems has gained in interest significantly. Most of these works concern aluminum toxicity. In general, the toxic effects of aluminum result from its competition with other metal ions in enzymes and proteins.[8] As the aluminum ion substitutes at the normal metal binding site, the function of the protein changes and alters the metabolism of the cell,[8] and consequently gravely affects the organism. MacDonald and Martin showed that the functions of magnesium(II) more than any other metal are affected by the competition with aluminum(III).[9,10]

The nervous system is especially susceptible[7] in humans. Alzheimer's disease, dialysis encephalopathy, and Parkinson-dementia complex of Guam are some examples of maladies linked to aluminum(III) interference. Recently, Fasman's group reported two mechanisms[11] for aluminum(III) interactions with the Neurofibrilar peptide (NF), in which aluminum may bind to carboxylate residues, forming *intrachain* complexes, or to phosphorilated residues of the NF, where *interchain* bonds are created.

In addition to magnesium(II), iron(III)[12] and calcium(II)[13−15] are also susceptible to competition with aluminum(III). Size similarity is a dominant factor over the charge identity concerning metal ion competition.[3,16] Thus, aluminum(III) substitution for magnesium(II), calcium(II), or iron(III) in physiological settings is possible. Magnesium(II) is the simplest metal that competes with aluminum(III). Thus, in this work we focus on the competition between magnesium(II) and aluminum(III).

The interactions of some metals with biologically relevant model ligands have been studied with ab initio methods, e.g., magnesium(II), calcium(II), cadmium(II), and zinc(II).[17−19] In these works, the amino acids are reduced to their functional groups, i.e., $HCOO^-$ for glutamic acid and aspartic acid, CH_3O^- for serine, CH_3SH for cysteine, etc. Magnesium(II) metal ion has also been studied in model protein environment with different bioligands, again representing the amino acids.[20] Despite the quantity of these relevant theoretical works and the extensive experimental study concerning aluminum interacting with these biologically relevant ligands, no ab initio work exploring these critical features has yet appeared in the literature.

Our hope in this investigation is not only to elucidate binding characteristics in these complexes but also to provide detailed data (see Supporting Information) that may be useful to develop force fields for aluminum, thereby facilitating molecular modeling studies that may be helpful to study the biotoxicity of aluminum.

To understand better the interactions of aluminum(III) with any relevant biological peptide, it is important to analyze first the interactions of the metal with the amino acids. In the present work he have studied the binding properties of magnesium(II) and aluminum(III) with the acidic amino acid chains aspartic and glutamic acids. To do so, first we have reduced the amino acids to their simplest functional group, i.e., the carboxylate anion. To extend the applicability of this study, we have also introduced the corresponding methyl groups to represent more accurately the side chain of these amino acids, i.e., $CH_3\,COO^-$ for aspartic acid $CH_3\,CH_3\,COO^-$ for glutamic acid. The amino acid chain has been represented in the anionic form because both amino acids p*K*'s are lower than the physiological pH.

With the data provided on this work, a better understanding of the interactions between the aluminum(III) cation and the carboxylate containing residues will be obtained, along with data that should be useful in the creation of force field parameters for the aluminum(III) cation.

2. Methods

All calculations were carried out with the GAUSSIAN94[21] package. Density functional methods have proven to give excellent results in most chemical systems,[22] with results comparable to those given by CPU intensive electron-correlation methods. However it frequently overestimates bond dissociation energies.[23] The hybrids of HF and DFT theories increment the accuracy of the dissociation energy as was validated by Johnson *et al.*[24] The Becke proposed hybrid[25] (B3), combined with the correlation functionals reported by Lee, Yang, and Parr,[26] (LYP) has been chosen for this work.

An all-electron 6-31G split valence basis set was used for each metal, and the relativistic compact effective core potentials

S1089-5639(98)01146-3 CCC: $15.00
Published on Web 08/11/1998

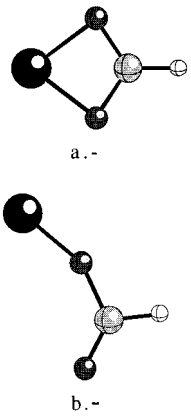

Figure 1. (a) Bidentate binding of the metal with the ligand. (b) Unidentate binding of the aluminum(III) cation with the ligand.

of Stevens *et al.*[27] were used with their corresponding 31 split valence basis sets for all other atoms. The basis set for each atom was augmented with a diffuse sp-set of functions and a polarization set of p- and d-functions. We shall refer to this basis as DZ+*.

To analyze the interactions of the aluminum(III) cation with the carboxylate residues, natural bond orbital[28] analysis was performed on the polyatomic wave function[29] using the NBO program[30] of the GAUSSIAN package. This method localizes the molecular orbitals and provides data that are in good agreement with the concepts of Lewis structures and the basic Pauling−Slater−Coulson picture of bond hybridization and polarization. For a good review of NBO and its applications, see the review article by Reed, Curtis, and Weinhold.[28]

The MOLDEN, visualization of molecular and electronic structure, program[31] was used for the depiction of the molecular orbitals (see Figures 2−7).

3. Results and Discussion

Our first representation of the acid amino acids corresponds to the functional group of the acid chain, the carboxylate anion. We have studied the interactions of this anion with two metal cations: magnesium(II) and aluminum(III). Then we have added methyl groups to represent more accurately the aspartic acid and glutamic acid amino acid chains. All the Cartesian coordinates and NBO charges of the isomers of the metal-containing complexes discussed below along with the relevant frequencies of the X−OOC cycle are available as Supporting Information.

A. X−HCOO$^-$ Complexes. According to the Becke3LYP level of theory using the basis set described above, the carboxylate anion has a C_{2v} symmetry with C−O bond lengths of 1.270 Å and a ∠OCO bond angle of 130.3°. In terms of charge location, the NBO[30] analysis reports the following: −0.844 e$^-$ of charge on the oxygen atoms and +0.702 e$^-$ of charge on the carbon atom.

The metals we have studied present two different orientations when binding to the carboxylate anion, unidentate and bidentate, the former being much higher in energy. The different structures characterized in this section are shown in Figure 1, and the important geometrical parameters are given in Table 1.

In the case of bidentate bonding, the metal, both oxygens, and the carbon form a planar cycle with C_{2v} symmetry. For the aluminum complex, the Al−O bond distance is 1.810 Å. There are significant changes in the geometry of the HCOO$^-$ fragment owing to this bonding to the cation. The C−O bonds lengthen by 0.041 Å to 1.311 Å and the ∠OCO angle shrinks by 15.5° with a final value of 114.8° to accommodate the bidentate bonding.

TABLE 1: Geometrical Figures of the X−OOCY Complexes Which Maintain the Symmetry of the COO−X Cycle, Where X = Al, Mg, and Y = H, CH_3, and CH_2CH_3

Y	X	X−O	C−O	∠OCO
H			1.270	130.0
	Al	1.809	1.311	114.8
	Mg	1.963	1.292	119.3
CH_3			1.272	128.8
(staggered isomer)	Al	1.788	1.332	112.2
	Mg	1.944	1.304	117.2
CH_2CH_3			1.273	128.7
(staggered isomer)	Al	1.813	1.318	113.3
	Mg	1.942	1.305	117.0

TABLE 2: NBO Charges of the X−OCCY Complexes That Maintain the Symmetry of the COO−X Terminus, Where X = Al, Mg, and Y = H, CH_3, and CH_2CH_3

Y	X	X	O	C
H			−0.844	0.702
	Al	2.349	−0.734	0.776
	Mg	1.767	−0.847	0.721
CH_3			−0.842	0.841
(staggered isomer)	Al	2.295	−0.766	0.933
	Mg	1.944	−0.870	0.890
CH_2CH_3			−0.844	0.841
(staggered isomer)	Al	2.145	−0.756	0.932
	Mg	1.748	−0.874	0.894

For the magnesium complex there are numerous signals of weaker metal−oxygen bonding. The Mg−O bond length at 1.963 Å is 0.154 Å longer than the Al−O bond (the covalent radius of magnesium is only 0.12 Å larger than that of aluminum), and the effect of complexation on the C−O bond length is much smaller; the C−O bond is lengthened by only 0.029 Å in the magnesium case. Clearly, to support bidentate bonding the ∠OCO angle must shrink substantially from its value in the free anion, but there again the magnesium cation causes less effect than the aluminum cation, the final ∠OCO angle being 119.3°.

Previous calculations by Garmer and Gresh[17] reported an Mg−O distance of 1.94 Å, at HF level of theory, with a 6-631G-(2d) basis set for magnesium(II) cation and SBK-31(2d) for the ligand atoms, and geometry optimizations performed with fixed ligand geometries. A slightly more recent work by Deerfield II et al.[20] reported a distance of 1.933 Å calculated at the HF/6-31++G** level of theory. Additionally, we have performed MP2/6-31++G** calculations with the magnesium−carboxylate complex. This level of theory predicted a value of 1.982 Å for the Mg−O bond length, while the B3LYP with the basis described above estimates a bond length of 1.963 Å. From this result we consider that our standard level of theory reproduces these systems with reasonable accuracy.

An interesting comparison between the two cases can also be made by examining the natural charges as given by the NBO analysis (see Table 2). The aluminum(III) cation in complexing with the carboxylate anion has a final natural charge of +2.349 e$^-$, decreasing the negative charge on the oxygen atoms to −0.734 e$^-$, and increasing the positive charge on the carbon atom to +0.776 e$^-$. The magnesium(II) cation receives only −0.233 e$^-$ worth of charge from the anion upon complexation, a charge transfer only slightly more than one-third that seen in the case of aluminum(III). Also of note in the Mg−OOCH]$^+$ complex is that the negative charge on the oxygen atoms is actually increased upon complexation, though only very slightly

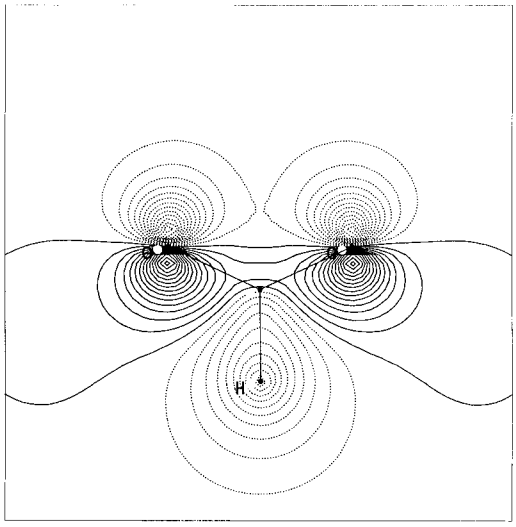

Figure 2. HOMO orbital of the carboxylate ($^-$OOCH) anion, which corresponds to the oxygen in-plane p-lone pairs.

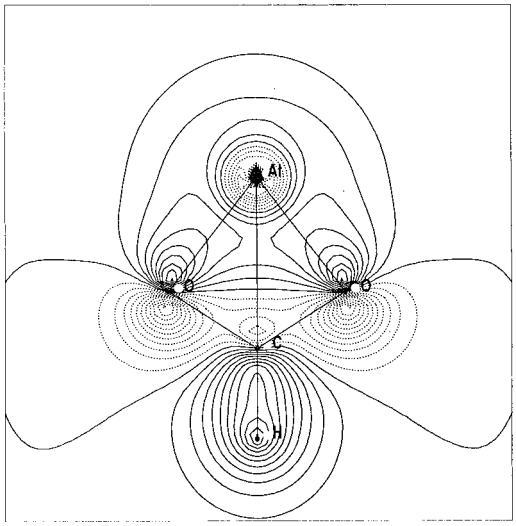

Figure 3. $7a_1$ orbital of the $Al-OOCH]^{2+}$ complex (HOMO-2), showing donations from the in-plane oxygen lone pairs to an empty s-orbital of the aluminum.

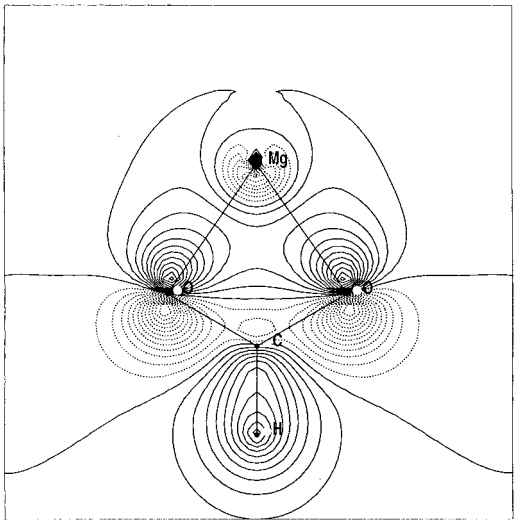

Figure 4. $7a_1$ orbital of the $Mg-OOCH]^{+}$ complex (HOMO-2), showing donations from the in-plane oxygen lone pairs to an empty s-orbital of the magnesium.

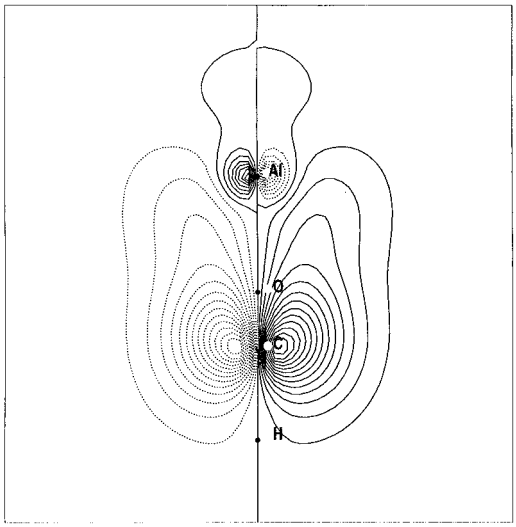

Figure 5. $2b_1$ orbital (HOMO-3), which is out of the O−C−O plane. In this orbital, donation of the carboxylate π-system into an empty aluminum p-orbital is observed.

(-0.847 e$^-$), and the positive charge on the carbon atom increases slightly to $+0.721$ e$^-$. In examining the molecular orbitals for these systems, we find that the main $HCOO^-$ cation interaction originates from the HOMO of the $HCOO^-$ moiety (Figure 2), which is one of the two in-plane oxygen lone pair orbitals. Donation is from this molecular orbital into the empty s-orbital of the metal cation. This is easily appreciated through inspection of Figures 3 and 4. The relative stregth of the interactions is also evident in these figures, the aluminum case (Figure 3) showing much larger metal participation than the magnesium case (Figure 4).

Other interactions between the two fragments can also be found. Figures 5 and 6 demonstrate the donation from the π-system of the $HCOO^-$ fragment into an empty p-orbital of the metal. These two figures are out-of-plane cuts along the C−M axis with the oxygen atoms above and below the plane. Again it is obvious that the aluminum(III) cation attracts more electron density than does the magnesium(II) cation. In the aluminum case, yet another interaction is worthy of note. The second in-plane oxygen lone pair molecular orbital is stabilized by donation into the in-plane p-orbital of aluminum (see Figure 7). This interaction can be found in the case of magnesium also, but the stabilization is minimal and the orbital that corresponds to Figure 7 is, in this case, the HOMO while the HOMO of the aluminum complex is the out-of-plane oxygen lone pair orbital.

The NBO analysis agrees with this picture. It reports one bond between the aluminum atom and each of the carboxylate's oxygen atoms. The bonds are formed by an in-plane sp_y aluminum hybrid and the oxygen in-plane p-orbitals. These orbitals are centered mainly on the oxygen atoms, but they also have a participation from aluminum of 11.75% which is enough, according to the NBO program, to be reported as a bond. Examining the second-order interactions, the most energetic are between the Al−O bonding orbitals and their opposite Al−O antibonding orbitals, each of these having energy of 13.75 kcal/mol.

The NBO analysis localizes the π-system of the carboxylate anion showing a lone pair on O_1 and a $C-O_2$ π-bond. Donations from these localized orbitals into the out-of-plane p-orbital of aluminum have energetic values of 7.73 and 8.21 kcal/mol, respectively, giving a numerical value to the $\pi \rightarrow$ p-orbital donation witnessed in Figure 5. The interactions

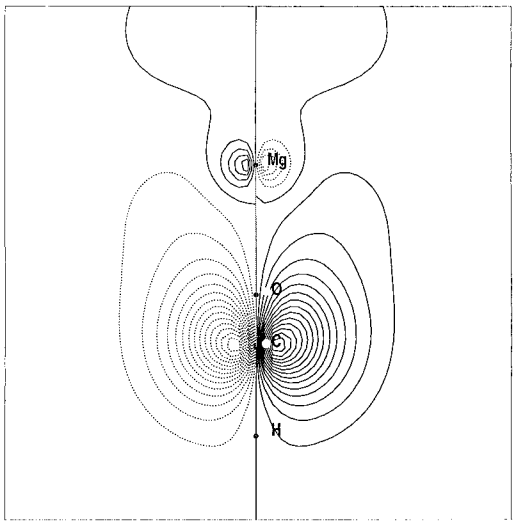

Figure 6. $2b_1$ orbital (HOMO-3), which is out-of the O−C−O plane. In this orbital, donation of the carboxylate π-system into an empty magnesium p-orbital is observed.

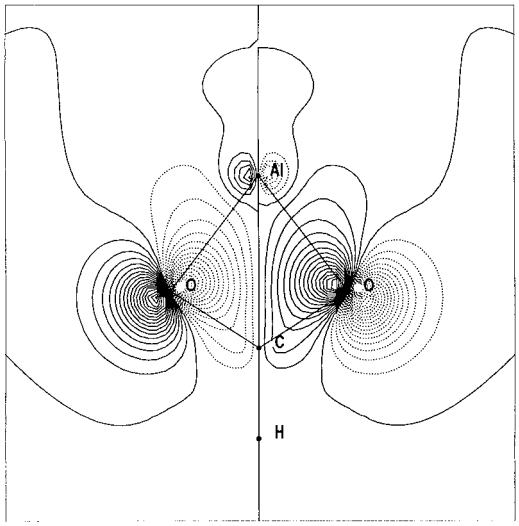

Figure 7. $2b_2$ (HOMO-1) orbital of the $Al-OOCH]^{2+}$ complex, demonstrating a donation from the second in-plane oxygen lone pair orbital into an aluminum in-plane p-orbital.

between the two in-plane oxygen lone pairs with the empty p-orbital of the aluminum atom have values of 3.27 kcal/mol each.

In addition to these interactions that are observed by looking at the MO's, some other interactions are reported by the NBO analysis such as a donation from the σ_{C-O} orbital to the opposite σ^*_{Al-O} antibonding orbital, as a consequence of the localization of the Al−OOC cycle, where each bond donation contributes 5.32 kcal/mol. Finally, the NBO analysis reports interaction between both Al−O bonding orbitals and the C−H antibonding orbital, with an energetic contribution of 8.52 kcal/mol.

For the magnesium complex, the NBO analysis does not show any bond per se between the magnesium(II) and the carboxylate moiety. Instead the NBO analysis reports that magnesium(II) and carboxylate units are held together by second-order interactions, which are in accordance with the molecular orbitals described above. The most important interactions are donations from the in-plane oxygen p-orbital lone pairs to the magnesium empty 3s-orbital with a energy contribution of 20.92 kcal/mol. These interactions are analogous to those that are given as Al−O bonds in the $AlOOCH]^{2+}$ case except that in this case the participation of the metal is not large enough for these to be considered bonds in the NBO report.

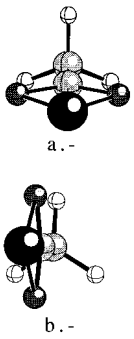

Figure 8. Staggered (a) and eclipsed (b) $X-OOCCH_3$ isomers.

More evidence of weaker $Mg-OOCH]^{+}$ interaction is that the donation from $C-O_2$ π bond into the magnesium p-orbital has an energy of only 2.31 kcal/mol, and the O_1 out-of-plane lone pair donation contributes only 2.22 kcal/mol (corresponding values were 8.21 and 7.73 kcal/mol in the aluminum complex). Also the oxygen in-plane lone pair donations to the magnesium in-plane p-orbital has an energy of only 2.71 kcal/mol. All of these interactions are weaker their corresponding interactions in the aluminum complex.

Following the molecular orbital and NBO analysis, it is certainly expected that the aluminum(III) interaction with the carboxylate anion would be much stronger than that of magnesium(II). While the magnesium−carboxylate interaction energy is −364.37 kcal/mol, the aluminum(III) interaction energy is −710.21 kcal/mol. Garmer and Gresh also reported a binding energy for the $Mg-OOCH]^{+}$ complex of −362.7 kcal/mol, which agrees with ours.

Another type of binding between aluminum(III) cation and the carboxylate anion was also found, where the metal cation binds only to one oxygen of the carboxylate. This bond length is 1.698 Å and has an angle ∠AlOC of 156.2°. There is a charge transfer to the aluminum atom of aproximately 1 e^- in this isomer. The natural charge on aluminum atom in this unidentate case is +2.089 e^-. The oxygen that binds the aluminum atom has a natural charge of −1.046 e^-, while the other oxygen only supports a charge of −0.162 e^-. The carbon atom has a natural charge of +0.768.

According to the NBO theory, the Al−O bond in this monodentate complex is a σ bond between the s-orbital of the aluminum and an oxygen in-plane p-orbital. The contribution of the aluminum in this bond is 31%, while its contribution was around 11% per bond for the bidentate complex. The second-order interactions are important in this complex and stronger than they were in the bidentate case. The most important donation is that of the σ^*_{Al-O} to the σ^*_{C-O} orbital with an energy contribution of 35.30 kcal/mol. The donation from one of the oxygen's in-plane lone pairs to an empty aluminum in-plane p-orbital has an energetic value of 29.17 kcal/mol. This oxygen lone pair also donates some charge to the σ^*_{Al-O} orbital, contributing 26.72 kcal/mol. The binding energy of the unidentate binding is only 26 kcal/mol lower than the aluminum-(III) bidentate binding mode; it has an energy of 684.41 kcal/mol.

B. X^{-} $OOC-CH_3$. A methyl group was added to the carboxylate anion for the appropriate simulation of the side chain effect of the aspartic acid amino acid. Then the interactions with the metal cations were studied, and the various complexes encountered are shown in Figure 8.

Two structures have been characterized at the B3LYP/DZ+* level of theory, both with C_s symmetry. One shows an eclipsed structure between one of the oxygens with respect to one of the methyl hydrogens, and the other staggered. These structures are nearly energetically degenerate with a difference of less than 0.1 kcal/mol. However, at the employed level of theory, the staggered isomer presents one small imaginary frequency (32*i* cm^{-1}) implying that the structure is a transition state for methyl group rotation.

The geometrical and energetic aspects of both structures are very similar; the main difference is the loss of the equivalence of the oxygens at the eclipsed structure. Thus, the C_{2v} symmetry of the COO residue is lost. In the eclipsed isomer, the C−O bonds differ by only 0.001 Å and the NBO charge distribution on the oxygen atoms differ by 0.009 e^-. The COO residue of the staggered isomer maintains the symmetry, where the C−O bond distance is 1.272 Å and the charge of the oxygens −0.842 e^-. The ∠OCO angle is the same for both isomers (128.9°).

When compared to the simple carboxylate anion, these structures show minor differences caused by the substitution of the terminal hydrogen with a methyl group. The ∠OCO angle shrinks a bit, and the C−O bonds are very slightly lengthened. The negative charges of the oxygen atoms are minutely lower, but the carboxylate carbon atom supports a positive charge 0.139 e^- greater when the methyl substitution is made.

Two different isomers were also located for each metal complex, with the conformations analogous to those of the CH_3COO^- ligand. In the case of aluminum complexation, the eclipsed isomer is now the transition state and the staggered isomer the minimum. However, the difference in energy is negligible, and the imaginary mode of the eclipsed isomer has a frequency of only 37*i* cm^{-1}. Thus we conclude that the methyl group is essentially a free rotor. For magnesium complexation, it turns out that both eclipsed and staggered isomers are local minima and again energy differences are negligible. For simplicity we will discuss the characteristics of the staggered isomers that maintain symmetry in the ring. Electronic and geometrical structure difference are minimal between isomers, and their charges and Cartesian coordinates are available in the Supporting Information.

The effect of the methyl electron donor group makes the anion bind more strongly to the metal cation owing to the polarization energy. Thus the binding energy for aluminum and magnesium are −741.91 and −375.25, kcal/mol, respectively, 30 and 10 kcal/mol stronger than the previously described X−OOCH bonding. Reflecting the binding energy increase, the X−O distances shrink and the C−O bonds lengthen. The Al−O bond distance is 0.009 Å shorter than in the $Al-OOCH]^{2+}$ complex. The C−O bond distance for the staggered isomer is 0.021 Å longer than in the simpler complex.

The charge distribution of the Al−OOC cycle changes slightly in comparison with the Al−carboxylate complex. The main difference is observed at the carbon atom which increases in charge by +0.157 e^-, with a new charge of +0.933 e^-. The aluminum and both oxygens gain some negative charge, with final values of +2.295 and −0.766 e^-.

Similar geometrical trends were observed for $Mg-OOC-CH_3]^+$ complexes. In this case, both isomers are stationary points. The C−O and Mg−O distances in the staggered complex are 1.304 and 1.944 Å, respectively, again longer and shorter than the same bonds in the unsubstituted case. The ∠OCO bond angle is also slightly smaller than it was in the unsubstituted case, though the change (−2.1°) is a bit less than it was in the Al case (−2.6°).

The NBO analysis, as it did at the previously studied complexes, only reports a bond per se between the aluminum(III) cation and the ligand, not between the magnesium(II) cation and the ligand. According to the NBO model, the different isomers of the present complex present few differences. The only remarkable point is that the oxygens of the ring lose their symmetry in the eclipsed isomer. However, their contributions are very similar, and also similar to the staggered isomer. Thus, again, we will stick to the staggered isomer in our analysis.

The aluminum contribution in the Al−O bond is slightly larger than it was in the $Al-OOCH]^{2+}$ complex, with an average participation of 12.18%. The second-order interactions are also important in these complexes. The strongest ones are the interactions between the σ_{Al-O} and the opposite σ^*_{Al-O} orbital, with a contribution close to 13 kcal/mol. As we saw before, the NBO analysis localizes the π-system, and the second-order interactions stabilize this complex by about 16.45 kcal/mol summing the π and out-of-plane lone pairs donations to the empty out-of-plane p-orbital of aluminum. This stabilization is 0.51 kcal/mol more than it was in the simple carboxylate−Al complex.

The C−C bond also participates in stabilizing the complexes, by facilitating the polarization of electron density. The σ_{C-C} bond donates some electronic density to each of the σ^*_{Al-O} antibonding orbitals, with an energetic contribution of 3.65 kcal/mol. The σ^*_{C-C} antibonding also receives some electronic contribution from each of the σ_{Al-O} bonding orbitals, with a higher energetical contribution: 11.52 kcal/mol in the staggered complex. A similar effect was observed between the σ_{Al-O} bonding and the σ^*_{C-H} antibonding orbitals of the $Al-OO-CH]^{2+}$ complex, but here the energetic contribution is larger.

Apart of the X−O bonds, the same trends are observed at the magnesium complex. Again the magnesium s-orbital participation is not large enough to be reported as a Mg−O bond, and the Mg−O connection appears in the second-order interactions. As they were in the $Mg-OOCH]^+$ complex, the oxygen p-lone pair orbital donations to the Mg empty 3s-orbital are the most important. The two oxygen in-plane p-lone pair donations contribute a total of about 40 kcal/mol, while this contribution was close to 42 kcal/mol at the unsubstituted complex. These oxygen lone pairs also donate some density to the magnesium in-plane empty p-orbitals, with an energetic contribution between 2.70 and 2.30 kcal/mol.

Finally, we mention that the C−C bond also contributes slightly stabilizing these complexes, but since there is no localized Mg−O bond in the NBO report, the interactions are reported to occur directly with the magnesium atom. The magnesium 2s-lone pair donates electronic density to the σ^*_{C-C} antibonding but only contributes 1.42 kcal/mol, and the σ_{C-C} bonding orbital interacts with the magnesium empty 3s-orbital contributing just 1.68 kcal/mol.

C. $X-^-OOC-CH_2CH_3$. Finally we have added a second methyl group to simulate more completely the glutamic acid amino acid chain. Various structures were found for each metal complex, and only the most interesting ones are shown in Figure 9 while other rotomers of the terminal methyl group are left out. All of these conformers are nearly energetically degenerate, their energy differences being less than 1.0 kcal/mol.

The isomer that maintains the C_{2v} symmetry of the OOC terminus will be referred to as conformation A. This isomer has one imaginary frequency, which corresponds to rotation of the CH_2CH_3 chain around the C−C bond. Conformers B with

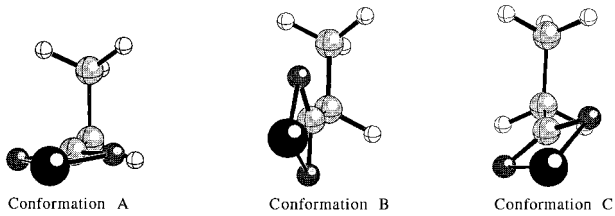

Figure 9. The three different conformations of $X-OOCCH_2CH_3$ complexes. **(**Conformation A) The oxygen atoms are staggered with the hydrogen atoms of the central carbon. (Conformation B) One oxygen atom is eclipsed with the terminal carbon. (Conformation C) One oxygen is eclipsed with a hydrogen of the central carbon.

C_s symmetry and C with only C_1 symmetry are local minima and lie 0.4 and 0.1 kcal/mol below conformer A, respectively. These three energetically quasi-degenerate isomers suggest that the carboxylate group is rotating more or less freely around the C−C axis.

As we have done in the previous section, we will focus again on the isomer that keeps the C_{2v} symmetry at the COO terminus in order to compare the results with the previously mentioned complexes. The Cartesian coordinates of all isomers are available as Supporting Information. The geometric characteristics of these complexes are very similar with those of the previously studied amino acid chains. The effect of adding a second methyl group follows the pattern set by the inclusion of the first methyl group to the carboxylate anion. The NBO charges are given in Table 2, where it can be seen that the charge distribution is very similar to that at the previous complex.

The interaction of the metals with the glutamic acid amino acid chain results in the analogous three complexes for each of the metal cations. One stable isomer with all positive frequencies and two stationary points with one imaginary frequency each were located. All these isomers are, again, essentially energetically degenerate lying within a range of 0.15 kcal/mol. The minimum corresponds to the previously described conformation A, which maintains the C_{2v} symmetry of the XOOC cycle. The other two isomers have one imaginary frequency corresponding to rotation of the aliphatic chain around the C−C bond axis. All of these complexes have very similar geometrical features, which may be found in the Supporting Information.

The addition of another methyl group increases the amount of charge transferred to aluminum (see Table 2) and changes the geometrical features of $Al-OOCH_3]^{2+}$ to values that are closer to the $Al-OOCH]^{2+}$ complex. There is a significant increase of the Al−O bond lengths, changing from 1.788 Å in the $Al-OOCCH_3]^{2+}$ complex to 1.813 Å in this $Al-OOCH_2-CH_3]^{2+}$ complex. Despite the elongation of the Al−O bond, the insertion of this new CH_3 group promotes stronger bonding between the aluminum(III) cation and the glutamic acid amino acid acid chain. This bonding has an energetic value of −754.03 kcal/mol, 12.12 kcal/mol stronger than the $Al-OOCCH_3]^{2+}$.

NBO analysis of the present complex follows a behavior similar to that of the previously analyzed aluminum(III) cation complexes. The second-order interactions are shown in Table 3. The most notable differences being that while the $\sigma_{Al-O} \rightarrow \sigma^*_{Al-O}$ donations are similar to those in the $Al-OOCH]^{2+}$ complex, the $\sigma_{Al-O} \rightarrow \sigma^*_{C-Y}$ are closer to the $Al-OOCCH_3]^{2+}$ complex. Additional interactions can be found in the Supporting Information.

Finally, we have located three different isomers with the previously described A, B, and C conformations of magnesium(II) cation interacting with the $^-OOCCH_2CH_3$ ligand. In this case, we have only one minimum, which corresponds to the conformation C. The other two isomers, as in the previously studied systems, are nearly isoenergetic with a negligible energy difference (less than 0.5 kcal/mol) and are transition states for rotation of the CH_2CH_3 chain around the C−C axis.

TABLE 3: Second-Order Interactions of the $Al-OOCY^{2+}$ Complexes That Maintain the Symmetry of the COO−X Cycle, Where Y = H, CH_3, and CH_2CH_3

interactions	H	CH_3	CH_2CH_3
$\sigma_{Al-O} \rightarrow \sigma^*_{Al-O}$	13.75	12.78	13.95
$\sigma_{Al-O} \rightarrow \sigma^*_{Al-O}$	13.75	12.78	13.95
$\sigma_{Al-O} \rightarrow \sigma^*_{C-Y}$	8.52	11.52	11.54
$\sigma_{Al-O} \rightarrow \sigma^*_{C-Y}$	8.52	11.52	11.54
$\pi_{C-O} \rightarrow n_{(Al3p_{out\text{-}of\text{-}plane})}$	7.73	7.86	5.62
$n_{(O2p_{out\text{-}of\text{-}plane})} \rightarrow n_{(Al3p_{out\text{-}of\text{-}plane})}$	8.21	8.63	6.45
$\sigma_{Al-O} \rightarrow \sigma^*_{C-O}$	5.32	4.73	4.57
$\sigma_{Al-O} \rightarrow \sigma^*_{C-O}$	5.32	4.73	4.57
$\sigma_{C-Y} \rightarrow \sigma^*_{Al-O}$	3.37	3.65	4.20
$\sigma_{C-Y} \rightarrow \sigma^*_{Al-O}$	3.37	3.65	4.20
$n_{(O2p_{in\text{-}plane})} \rightarrow n_{(Al3p_{in\text{-}plane})}$	3.27	2.24	1.74
$n_{(O2p_{in\text{-}plane})} \rightarrow n_{(Al3p_{in\text{-}plane})}$	3.27	2.24	1.74

TABLE 4. Second-Order Interactions of the $Mg-OOCY^+$ Complexes That Maintain the Symmetry of the COO−X Cycle, Where Y = H, CH_3, and CH_2CH_3

interactions	H	CH_3	CH_2CH_3
$n_{(O2p_{in\text{-}plane})} \rightarrow n_{(Mg3s)}$	20.92	19.93	20.12
$n_{(O2p_{in\text{-}plane})} \rightarrow n_{(Mg3s)}$	20.92	19.93	20.12
$\pi_{C-O} \rightarrow n_{(Mg3p_{out\text{-}of\text{-}plane})}$	2.31	2.01	1.94
$n_{(O2p_{in\text{-}plane})} \rightarrow n_{(Mg3s)}$	2.22	2.02	2.21
$n_{(O2p_{in\text{-}plane})} \rightarrow n_{(Mg3s)}$	2.82	2.80	2.84
$n_{(Mg2s)} \rightarrow n_{(Mg3s)}$	2.82	2.80	2.84
$\sigma_{C-Y} \rightarrow n_{(Mg3s)}$	1.09	1.68	1.76
$n_{(Mg2s)} \rightarrow \sigma^*_{C-H}$	0.52	1.42	1.33
$n_{(O2p_{in\text{-}plane})} \rightarrow n_{(Mg3p_{out\text{-}of\text{-}plane})}$	2.71	2.54	2.59
$n_{(O2p_{in\text{-}plane})} \rightarrow n_{(Mg3p_{out\text{-}of\text{-}plane})}$	2.71	2.54	2.59

Again, we focus our discussion into the isomer with conformation A, which maintains the symmetry at the Mg−OOC ring. In this case, the effect of the inclusion of the second methyl group is not as important as it was at the aluminum complexes; the geometrical patterns we have been following so far are nearly unchanged in comparison with the $Mg-OOCCH_3]^+$ complex. The change of the natural charges is also smaller than that in the aluminum complexes.

The second-order interactions of this complex are shown in Table 4, and comparing with the previous complexes interactions, we see that these interactions are almost unchanged whether we compare with the $Mg-OOCH]^+$ or the $Mg-OOCCH_2CH_3]^+$ complexes. The most remarkable difference is that there are new small second-order interactions in which each oxygen sp-in-plane hybrid donates some electronic density to an empty magnesium sp-in-plane orbital, having an energy contribution of 1.33 kcal/mol each.

It is clear that the effect of the second methyl group is not as important as it was for the aluminum complexes comparing both the geometrical and natural charge trends. The effect is also much smaller in the binding energy between the magnesium(II) cation and the glutamic acid amino acid chain. This energy has a value of −376.36 kcal/mol, which is only 1.1 kcal/mol stronger than that of the magnesium(II) cation complex with the aspartic acid amino acid chain.

4. Conclusions

In this work, we have studied the interactions between the aspartic acid and glutamic acid amino acid residues, with the aluminum(III) and magnesium(II) metal cations. First we studied the interactions between the smallest functional group of both amino acids (the carboxylate anion) with both cations.

After that, we sequentially introduced methyl groups to simulate more accurately the complete acid chain of the aspartic acid amino acid and the glutamic acid amino acid chain. The additional methyl groups are essentially free-rotor systems, and our analysis focused on isomers with higher symmetry. The Supporting Information contains complete geometry and vibrational frequency data for each stationary point located in this study. It is our hope that these data will assist the development of improved force fields for molecular dynamics investigations of aluminum biotoxicity.

The addition of a first methyl group stabilizes both metal complexes, but this effect is significantly larger for the aluminum(III) complex. The addition of a second methyl group stabilizes the complexes yet again, but the effect is reduced significantly, especially in the case of magnesium(II).

We have also performed the NBO analysis on these complexes. The NBO analysis locates a bond between the aluminum(III) and the three different ligands but characterizes the magnesium bonding as due the second-order interactions. The participation of the metal in the bonding is increased as methyl groups are added, as do the energetic values of the second-order interactions.

Acknowledgment. J.M.M. and J.E.F. thank the Basque Government (Eusko Jaurlaritza) for a grant. Financial support from the Spanish DGICYT Grant No. PB96/1524 and from the Provincial Government of Gipuzkoa (Gipuzkoako Foru Aldundia) is gratefully acknowledged.

Supporting Information Available: Tables 1−11 containing complete geometry and vibrational frequency data for stationary points in this study (11 pages). Ordering and access information is given on any current masthead page.

References and Notes

(1) Cotton, F. A.; Wilkinson, G. *Advanced Inorganic Chemistry*; Oxford University Press: New York, 1989.
(2) Silva, J. J. R. F. D.; Williams, R. J. P. *The Biological Chemistry of Elements*; Clarendom Press: Oxford, 1991.
(3) Martin, R. B. *Clin. Chem.* **1986**, *32*, 1797−1806.
(4) Williams, R. J. P. *Coor. Chem. Rev.* **1996**, *149*, 1−9.
(5) Birchall, J. D.; Exley, C.; Chappell, J. S.; Philips, M. J. *Nature (London)* **1989**, *146*−*148*, 338.
(6) Goyer, R. A. *Annu. Rev. Nutr.* **1977**, *17*, 37.
(7) Meiri, H.; Banin, E.; Mical, R.; Rosseu, A. *Prog. Neurobiol.* **1993**, *44*, 89−121.
(8) Birchall, J. D. *Aluminum in Chemistry Biology and Medicine*; Wiley: New York, 1992.
(9) Macdonald, T. L.; Humphreys, W. G.; Martin, R. B. *Science* **1987**, *286*, 183−186.
(10) Macdonald, T. L.; Martin, R. B. *Trends Biochem. Sci.* **1988**, *13*, 15−19.
(11) Hollosy, M.; Shen, Z. M.; Perzel, A.; Fasman, G. *Proc. Natl. Acad. Sci. U.S.A.* **1994**, *91*, 4902−4906.
(12) Battistiuzzi, G.; Calzolai, L.; Messori, L.; Sola, M. *Biochem. Biophys. Res. Commun.* **1995**, *206*, 161−170.
(13) Nachshen, D. A. *J. Gen. Physiol.* **1984**, *83*, 941−964.
(14) Koening, M. L.; Jope, R. S. *J. Neurochem.* **1987**, *49*, 316−320.
(15) Meiri, H.; Shimoni, Y. *Br. J. Pharmacol.* **1991**, *102*, 483−491.
(16) Ganrot, P. O. *Environ. Health Perspect.* **1986**, *65*, 363−441.
(17) Garmer, D. R.; Gresh, N. *J. Am. Chem. Soc.* **1994**, *116*, 3556.
(18) Gresh, N.; Stevens, W. J.; Krauss, M. *J. Comput. Chem.* **1995**, *16*, 843.
(19) Gresh, N.; Garmer, D. R. *J. Comput. Chem.* **1996**, *17*, 1481.
(20) Deerfield II, D. W.; Fox, D. J.; Head-Gordon, M.; Hiskey, R. G.; Pedersen, L. G. *Proteins* **1995**, *34*, 5054.
(21) Frisch, M. J.; Trucks, G. W.; Schlegel, H. B.; Gill, P. M. W.; Johnson, B. G.; Robb, M. A.; Cheeseman, J. R.; Keith, T.; Petersson, G. A.; Montgomery, J. A.; Raghavachari, K.; Al-Laham, M. A.; Zakrzewski, V. G.; Ortiz, J. V.; Foresman, J. B.; Peng, C. Y.; Ayala, P. Y.; Chen, W.; Wong, M. W.; Andres, J. L.; Replogle, E. S.; Gomperts, R.; Martin, R. L.; Fox, D. J.; Binkley, J. S.; Defrees, D. J.; Baker, J.; Stewart, J. P.; Head-Gordon, M.; Gonzalez, C.; Pople, J. A. *Gaussian94 b.2*; Gaussian, Inc.: Pittsburgh, PA, 1995.
(22) Labanowsky, J.; Andelzelm. J. *Density Functional Methods in Chemistry*; Springer-Verlag: New York, 1991.
(23) Tschinke, V.; Ziegler, T. *Theor. Chim. Acta* **1991**, *81*, 651.
(24) Johnson, B. G.; Gill, P. M. W.; Pople, J. A. *J. Chem. Phys.* **1993**, *98*, 5612.
(25) Becke, A. D. *J. Chem. Phys.* **1993**, *98*, 5648.
(26) Lee, C.; Yang, W.; Parr, R. G. *Phys. Rev. B* **1988**, *37*, 785.
(27) Stevens, W. J.; Krauss, M.; Basch, H.; Jasien, P. G. *Can. J. Chem.* **1992**, *70*, 612.
(28) Reed, A. E.; Curtiss, L. A.; Weinhold, F. *Chem. Rev.* **1988**, *88*, 899.
(29) Foster, J. P.; Weinhold, F. *J. Am. Chem. Soc.* **1980**, *102*, 7211.
(30) Glendening, E. D.; Reed, A. E.; Carpenter, J. E.; Weinhold, F. NBO Version 3.1.
(31) For the MOLDEN program, see: http://www.caos.kun.nl/~schaft/molden/molden.html.